HYDROGEN PRODUCTION EFFECT ON MICROSTRUCTURE OF HFIR-IRRADIATED LOW ACTIVATION F82H STEEL USING ^{54}Fe ISOTOPE--

E. Wakai (Japan Atomic Energy Research Institute), N. Hashimoto (Oak Ridge National Laboratory), K. Shiba, Y. Miwa(JAERI), J. P. Robertson, and R. L. Klueh(ORNL)

OBJECTIVE

The purpose of the present study is to investigate the effect of hydrogen production on the microstructure and mechanical properties of ^{54}Fe-doped F82H steel irradiated in HFIR.

SUMMARY

Reduced-activation F82H-std and a similar F82H doped with ^{54}Fe (F82H(^{54}Fe)) steels were irradiated at 250°C to 2.8 dpa in HFIR and examined by TEM. The produced hydrogen concentration in the F82H(^{54}Fe) steel is estimated to be 68 appm. Pre-irradiation microstructures of F82H(^{54}Fe) steel were very similar to those of F82H-std steel. A few small cavities were formed in the irradiated F82H(^{54}Fe) steel, but the swelling is insignificant, while in the F82H-std steel no cavities were observed. Precipitates with contrast similar to α' phase were observed on many dislocation loops in these steels. The number density and mean size for dislocation loops in the F82H-std and F82H(^{54}Fe) steels are 1.4 x10^{22} m^{-3} and 7.9 nm, and 2.1x10^{22} m^{-3} and 6.6 nm, respectively. The types of loops are **b**=(**a**/2)<111> for the F82H-std and **b**=(**a**/2)<111> and **a**<100> for the F82H(^{54}Fe) steel. The concentration of **a**<111> type to all loops in the F82H(^{54}Fe) steel is about 73%.

PROGRESS AND STATUS

1. Introduction

Ferritic/martensitic steels are candidate materials for the first wall and blanket structure of fusion reactors. In the D-T fusion reaction, the high-energy neutrons produced induce displacement damage and generate hydrogen and helium gas atoms in the materials from (n, p) and (n, α) reactions. The presence of these gases could lead to degradation of mechanical properties. In order to investigate the effect of hydrogen gas atoms on ferritic steels using a fission reactor, hydrogen gas atoms can be generated in F82H by doping with the ^{54}Fe isotope. Irradiation of such an alloy in a mixed-spectrum fission reactor with thermal neutrons like the High Flux Isotope Reactor (HFIR) results in the following transmutation reactions:

^{54}Fe(n, p)^{54}Mn,

^{54}Fe(n, α)^{52}Cr.

The effects of neutron irradiation on the tensile deformation of F82H steel have been reported. Shiba et al. [1-2] have described the tensile data, obtained under the U.S. DOE/JAERI program, following irradiation in HFIR at 200 to 600°C for doses in the range 3-34 dpa; The effect of helium production on mechanical properties were investigated using an isotope of boron (^{10}B). A summary of the tensile data for 9-12Cr ferritic/martensitic steels irradiated under a variety of

conditions has been presented by Rowcliffe et al. [3] and Zinkle et al.[4]. Klueh et al. [5] have reported that DBTT shifts of F82H-std, OPTIFER-1a, and 9Cr-2WVTa steels increase for irradiation temperatures below 300°C even for low damage levels of 1-3 dpa.

The purpose of the present study is to analyze the radiation-induced microstructural changes under hydrogen production in the ^{54}Fe-doped F82H steels.

2. Experimental procedure

The chemical compositions of the F82H-std and F82H(^{54}Fe) specimens used in this study are given in Table 1. The mass ratio of iron for these specimens was analyzed to be as shown in Table 2, correcting for the presence of ^{54}Cr. This means that about 96 % of iron atoms in the doped alloy were composed of ^{54}Fe in the F82H(^{54}Fe) specimen [6]. Normalizing and tempering were performed in a vacuum followed by air-cooling as given in Table 3. The details of the preparation process for the F82H(^{54}Fe) is described in ref. [6].

Table 1 Chemical compositions of the specimens used in this study (wt%)

Alloys	Cr	B	C	N	P	S	Al	Si	V	Mn	Ta	W
F82H-std	7.46	0.0004	0.094	0.002	0.003	0.003	0.019	0.09	0.18	0.07	0.03	2.1
F82H(^{54}Fe)	7.1	-	0.097	0.007	<0.002	0.0015	0.03	0.55	0.15	0.40	0.04	1.8

Table 2 Mass ratio analysis of the isotopically tailored F82H steel using ^{54}Fe

Alloy	Relative mass ratio		
	54/56	57/56	58/56
F82H-std	0.083	0.023	0.0003
F82H(^{54}Fe)	40	0.0083	0.00087

Table 3 Heat treatment

Alloy	Normalizing	Tempering
F82H-std	1040°C, 0.67h	740°C, 2h
F82H(^{54}Fe)	1040°C, 0.33h	745°C, 0.67h

Table 4 Neutron fluence (n/cm^2) and damage value for the F82H steel

Total	Thermal (<0.5 eV)	0.5 eV - 0.1 MeV	> 0.1 MeV	> 1 MeV	Damage (dpa)
1.26×10^{21}	4.78×10^{21}	4.09×10^{20}	3.73×10^{20}	1.96×10^{20}	~2.8

Standard 3 mm-diameter disks punched from 0.25 mm-thickness sheet stock were irradiated in the HFIR target in the HFIR-MFE-JP17 capsule as part of the JAERI/US collaborative program. The irradiation began on December 31, 1991, at the start of HFIR fuel cycle 304 and ended February 27, 1992, at the end of HFIR cycle 305. The exposure for the irradiation was 3702 MWd, or approximately 43.6 days at 85 MW reactor power. The complete description and details of the design, construction, and installation of the capsule have been previously reported [7-9]. The irradiation temperatures and displacement damage were 250 °C and about 2.8 dpa for the F82H steel in the JP17 capsule. The neutron fluence data [10] are given in Table 4. Hydrogen and helium production in the F82H(^{54}Fe) steel irradiated to 2.8 dpa were estimated to be 68 appm H and about 1 or 2 appm He, respectively, using only a reference data for spectral averaged cross section (^{54}Fe(n, p) ^{54}Mn--1.19x10^{-2} barn, ^{54}Fe(n, α) -- (1.9 or 3.6) x10^{-4} barn) [11]. In the F82H-std steel, the values of hydrogen and helium production were also estimated to be 5 appm H and 5 appm He (4 appm He produced from impurity boron), respectively, using impurity boron concentration and the reference data (^{54}Fe(n, p) ^{54}Mn--1.19x10^{-2} barn, ^{56}Fe(n, p) ^{56}Mn--2.4x10^{-4} barn) [11].

Microstructures of these specimens were examined using a JEM-2000FX transmission electron microscope with a LaB_6 gun operated at 200 kV. Microstructures of unirradiated control specimens were also examined.

3. Results

3.1 Pre-irradiation microstructures of the F82H-std and F82H(^{54}Fe) steels

The microstructure after normalizing and tempering was a lath martensitic structure in both the F82H-std and F82H(^{54}Fe) steel, and these steels are very similar to each other as shown in Figs. 1(a) and 1(b). Large precipitates of $M_{23}C_6$ carbides were observed in the matrix and on grain boundaries in these steels. MC carbides also formed in the matrix for these steels. The dislocation density for the two steels was nearly equal. The mean width of the lath boundaries for the F82H(^{54}Fe) was close to that for F82H-std. The microstructural features are summarized in Table 5.

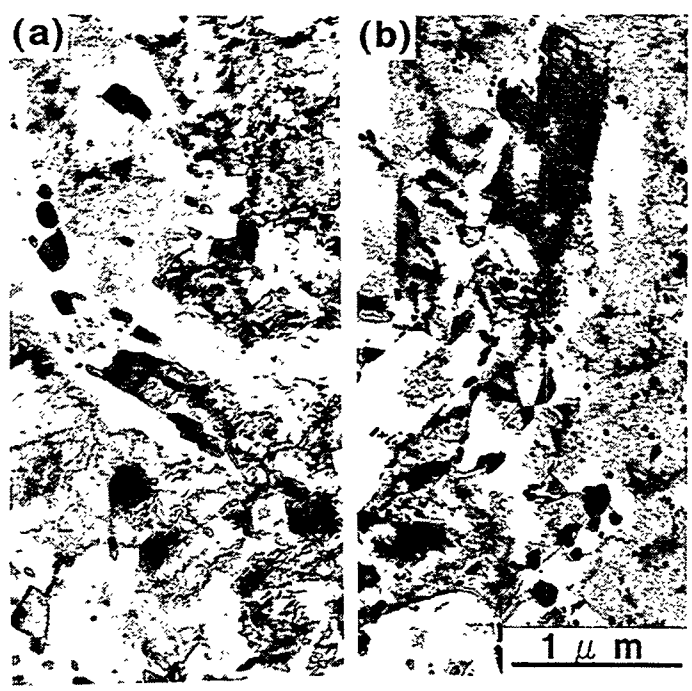

Fig. 1 Pre-irradiation microstructures of (a) F82H-std and F82H(^{54}Fe) steels

Table 5 Summary of defect clusters formed in the F82H and F82H(^{54}Fe) steels. RMC denotes root mean cube.

	F82H-std unirradiated	F82H(^{54}Fe) unirradiated	F82H-std 250°C, 2.8 dpa	F82H(^{54}Fe) 250°C, 2.8 dpa
Dislocation loops	-	-		
Number density			1.4×10^{22} m^{-3}	2.1×10^{22} m^{-3}
Mean size			7.9 nm	6.6 nm
Dislocations				
Areal number density	9×10^{13} m^{-2}	1×10^{14} m^{-2}	1×10^{14} m^{-2}	9×10^{13} m^{-2}
Cavities	-	-		
Number density			0 m^{-3}	5×10^{19} m^{-3}
RMC radius			0 nm	1.9 nm
Swelling			0 %	0.0001%
$M_{23}C_6$				
Number density	3×10^{20} m^{-3}	5×10^{20} m^{-3}	3×10^{20} m^{-3}	3×10^{20} m^{-3}
Mean size	62 nm	76 nm	73 nm	65 nm
MC				
Number density	$<1\times10^{20}$ m^{-3}	2×10^{20} m^{-3}	1×10^{20} m^{-3}	2×10^{20} m^{-3}
Mean size	14 nm	12 nm	13 nm	13 nm
Lath				
Mean width of lath	440 nm	480 nm	410 nm	450 nm

3.2 Standard F82H steel irradiated at 250°C to 2.8 dpa

Figures 2(a)-(c) show microstructures of the F82H-std steel irradiated at 250°C to 2.8 dpa; these micrographs were taken in the [001] direction using g=110 at a low and high magnification of bright-field image condition, and a high magnification of weak beam dark-field image condition, respectively. Dislocation loops were observed on {111} planes with (a/2)<111> Burgers vectors. Some loops were arranged along dislocation lines. The number density and mean size of the loops were 1.4×10^{22} m^{-3} and 7.9 nm, respectively. Precipitates with contrast like α'-phase were observed on many dislocation loops. A few MC carbides were observed in the matrix. No cavities were observed. The microstructural features are also summarized in Table 5.

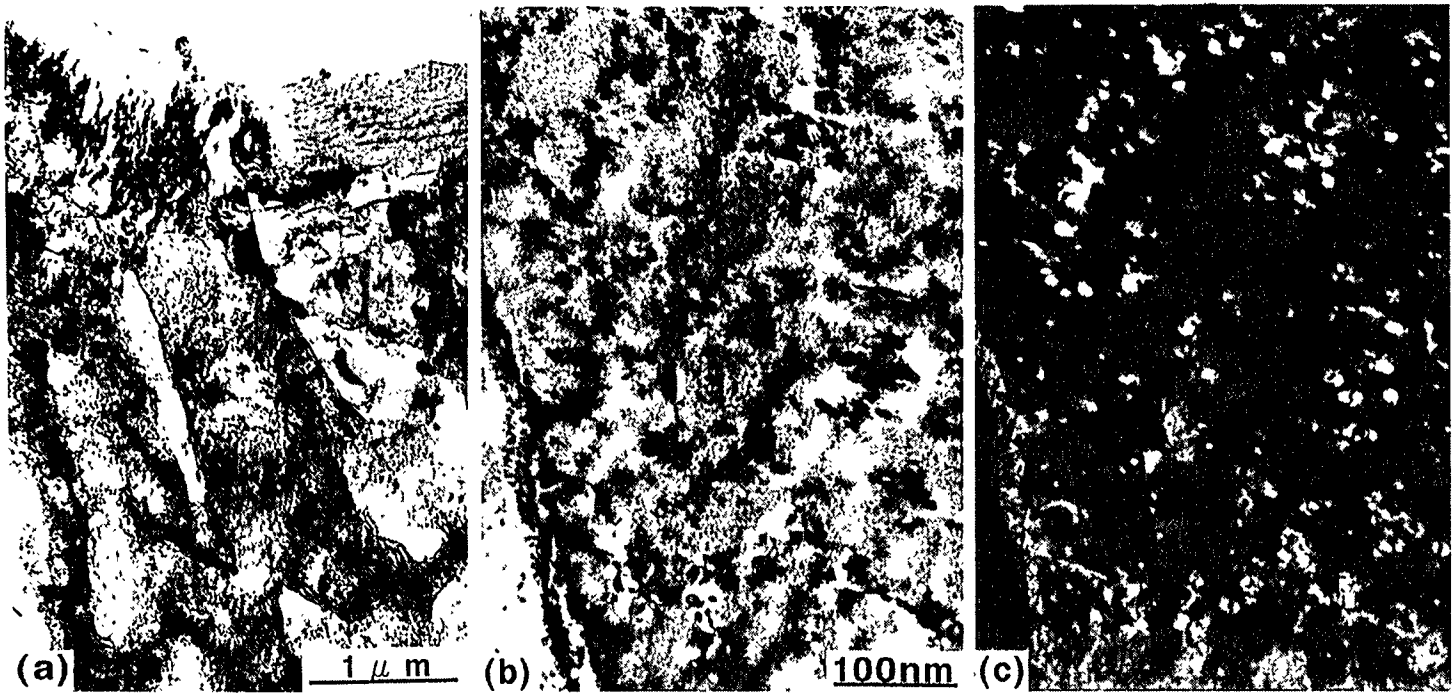

Fig. 2 Microstructures of (a) a bright-field image in low magnification, (b) a bright-field image in high-magnification, and (c) a weak beam dark-field image in high-magnification in the **F82H-std** steel irradiated at 250°C to 2.8 dpa. Precipitates with contrast like α'-phase are seen on many dislocation loops.

3.3 F82H(^{54}Fe) steel irradiated at 250°C to 2.8 dpa

Figures 3(a)-(c) show microstructures of the F82H(^{54}Fe) steel irradiated at 250°C to 2.8 dpa; these micrographs were also taken from the [001] direction using g=110 at a low and high magnification of bright-field image condition, and a high magnification of weak beam dark-field image condition, respectively. Two types of dislocation loops were observed: those on {111} planes with (a/2)<111> Burgers vectors and those on {100} planes with a<100> ones. The concentration of <111> type to all loops was about 73%. The total number density and mean size of loops was 2.1×10^{22} m^{-3} and 6.6 nm, respectively. Precipitates contrast like α'-phase were also observed on many dislocation loops. A few MC carbides were observed in the matrix. As shown in Fig. 4, several small cavities were observed, and the number density, root mean cube of radius, and swelling of cavities were 5×10^{19} m^{-3}, 1.9 nm, and 0.0001%, respectively .

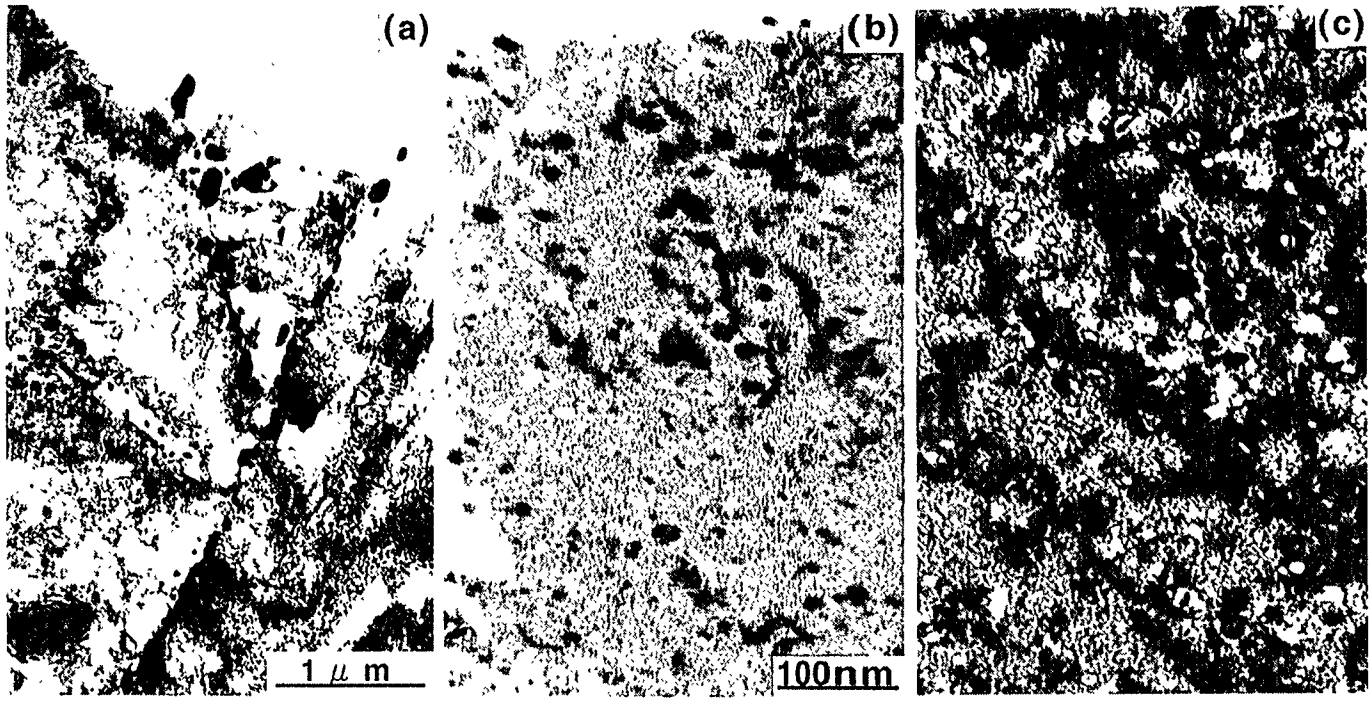

Fig. 3 Microstructures of (a) a bright-field image in low magnification, (b) a bright-field image in high-magnification, and (c) a weak beam dark-field image in high-magnification in the F82H(^{54}Fe) steel irradiated at 250°C to 2.8 dpa. Precipitates with contrast like α'-phase are also seen on many dislocation loops.

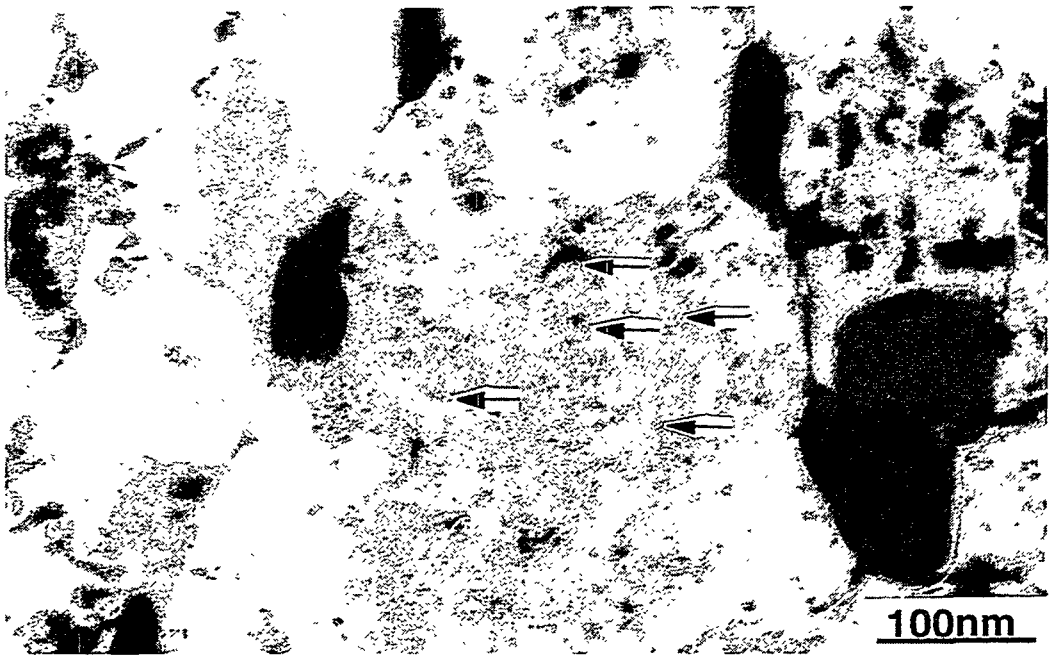

Fig. 4 Cavities formed in the the F82H(^{54}Fe) steel irradiated at 250°C to 2.8 dpa.

4. Discussion

4.1 Precipitates with contrast like α'-phase observed on dislocation

According to ref. [12-16] for radiation effects of binary Fe-(9-50)Cr alloys, dislocation loop formation was affected by the purity level of the alloys, and in many case Cr-rich-precipitates (α'-phase) on the loops were formed. Under 1 MeV electron irradiation, α' precipitate formation on dislocation loops was observed at temperatures below 600°C in an Fe-9Cr alloy. As the irradiation temperature decreased the dislocation loop density increased and α' precipitate density also increased. In case of neutron irradiation, the α' precipitate density on the dislocation loops was less than that in case of electron irradiation, and the cause of it may be considered to be due to cascades and low damage rates in the neutron environment. This formation of α' precipitate on dislocation loops in Fe-Cr alloys could cause large shifts of DBTT and large increases of yield strength (Y.S.), such as ΔDBTT = 145°C and Δ Y.S. = 260 MPa seen for high-purity Fe-9Cr alloys irradiated at 330°C to 0.3 dpa in JRR-3M (Modified Japan Research Reactor-3) [13, 14]. Therefore, the cause of the large shift of DBTT, +130°C, in the F82H-std irradiated at 250°C to 2.8 dpa [5] may be explained by the idea that the precipitates seen on dislocation loops in this experiment are α'-phase .

4.2 Type of dislocation loops

It is well known that the formation energy of (a/2)<111> loops is smaller than that of a<100> loops. Recently, purity effects of Fe-(9-50)Cr alloys, corresponding to 99.7% (including about 100 wt.ppm carbon) and 99.99% purity (including about 3 - 60 wt.ppm carbon), on dislocation loops under irradiation were investigated [12,16]. The number density of loops increased with increasing impurity level, such as carbon and nitrogen atoms, and the mean size of loops decreased with impurity level. The loops on {100} planes with a<100> Burgers vector were observed in all specimens. In addition to this, another type of loops on {111} planes with (a/2)<111> formed in high-purity Fe-Cr alloys. Carbon concentration was very sensitive to the type of loop formation, and no formation of (a/2)<111> type was in the Fe-Cr alloys with more than 60 wt.ppm carbon. The number ratio percentage of (a/2)<111> type to all types was about 60-70% at 300°C and 80-90% at 500 °C in the high-purity Fe-Cr alloys (including 3-5 wt.ppm carbon). These reference data suggest that the formation of a<100> type is very difficult in the higher purity Fe-Cr alloys with less than 3 wt.ppm carbon. F82H(^{54}Fe) steels irradiated at 250°C to 2.8 dpa have two types of loops of (a/2)<111> and a<100>, while F82H-std has only one type of (a/2)<111>. This results may be related to the free carbon concentration in the matrix. The tempering time for the former steel is shorter than that of F82H-std, and the carbide formation may not be saturated. Therefore, it can be considered that the free carbon concentration in the matrix in F82H-std steel may be very low.

ACKNOWLEDGMENTS

The authors would like to thank Drs. A. F. Rowcliffe and S. J. Zinkle in Oak Ridge National Laboratory and members of Radiation Effect Analyses Laboratory in Japan Atomic Energy Research Institute for fruitful discussions. We are also grateful to Messrs. L. T. Gibson, A. T. Fisher, and J. J. Duff, and the members of the Irradiated Materials Examination and Testing Laboratory of ORNL for technical supports.

REFERENCES

[1] K. Shiba, I. Ioka, J. P. Robertson, M. Suzuki, and A. Hishinuma, Euromat-9 6(1996), p.265.
[2] K. Shiba et. al, unpublished data.
[3] A. F. Rowcliffe, J. P. Robertson, R. L. Klueh, K. Shiba, D. J. Alexander, M. L. Grossbeck, and S. Jitsukawa, J. Nucl. Mater., 258-263(1998), pp. 1275-1279.
[4] S. J. Zinkle, J. P. Robertson, and R. L. Klueh, Fusion Reactor Materials Semiannual Progress Report for Period Ending June 30, 1988, Office of Fusion Energy, DOE/ER-0313/24, pp. 135-143.
[5] R. L. Klueh, D. J. Alexander, and M. Rieth, Fusion Reactor Materials Semiannual Progress Report for Period Ending June 30, 1988, Office of Fusion Energy, DOE/ER-0313/24, pp. 150-162.
[6] M. Suzuki, A. Hishinuma, N. Yamonouchi, M. Tamura, and A. F. Rowcliffe, J. Nucl. Mater., **191-194**(1992), pp. 1056-1059.

[7] A. W. Longest, D. W. Heatherly, K. R. Thoms, and J. E. Corum, Fusion Reactor Materials Semiannual Progress Report for Period Ending March 31, 1991, Office of Fusion Energy, DOE/ER-0313/10, p.3.
[8] A. W. Longest, D. W. Heatherly, J. E. Wolfe, K. R. Thoms, and J. E. Corum, Fusion Reactor Materials Semiannual Progress Report for Period Ending September 30, 1991, Office of Fusion Energy, DOE/ER-0313/11, p.30.
[9] A. W. Longest, D. W. Heatherly, K. R. Thoms, and J. E. Corum, Fusion Reactor Materials Semiannual Progress Report for Period Ending March 31, 1992, Office of Fusion Energy, DOE/ER-0313/12, p.24.
[10] L. R. Greenwood and C. A. Balwin, Fusion Reactor Materials Semiannual Progress Report for Period Ending March 31, 1996, Office of Fusion Energy, DOE/ER-0313/19, pp. 286-290.G. [11] R. Odette, J. N. Mater., **141-143**(1986), pp. 1011-1017.
[12] E. Wakai, A. Hishinuma, K. Yano, S. Takaki, and K. Abiko, J. Physique (IV) ,**5**(1995), C7-pp. 277-286.
[13] A. Hishinuma, E. Wakai, S. Takaki, and K. Abiko, Proc. Ultra High Purity Base Metals, 1998, pp. 27-34.
[14] E. Wakai, A. Hishinuma, S. Takaki, and K. Abiko, to be applied, in Proc. Ultra High Purity Base Metals, 1999.
[15] E. Wakai, A. Hishinuma, T. Sawai, S. Kato, S. Isozaki, S. Takaki, and K. Abiko, Phys. Stat. Sol. (a), **160**(1997), p.441.
[16] E. Wakai, A. Hishinuma, Y. Kato, S. Takaki, and K. Abiko, Proc. Ultra High Purity Base Metals, Eds. K. Abiko, K. Hirokawa, and S. Takaki, The Japan Institute of Metals Sendai (Japan), (1994), p.522.